Ionic Mechanisms of Triggered Activity in Atrial Cell Models

Marta Varela, Ross Morgan, Nooshin Ghavami, Stuart James, Oleg Aslanidi

Department of Biomedical Engineering, Division of Imaging Sciences & Biomedical Engineering, King's College London, St Thomas' Hospital, London, United Kingdom

Abstract

Spontaneous electrical activity in the atria, primarily near the pulmonary veins (PVs), is strongly linked with triggers for atrial fibrillation (AF). However, mechanisms of such triggered activity are incompletely understood. In this study, we use electrophysiologically detailed atrial cell models to investigate the role of late sodium current, I_{NaL}, in the mechanisms of triggered activity. The model simulations show that increases of this inward current (seen in several conditions that predispose to AF) can play a key role in the initiation of spontaneous diastolic depolarisation in atrial cells. Sustained triggered activity also requires contributions of other factors − increased L-type calcium current and decreased potassium currents − which are associated with β-adrenergic stimulation of atrial cells. The proposed mechanism is in agreement with experiments showing that triggered activity can be induced in the PVs primarily by β-adrenergic stimulation and stopped by ranolazine, a blocker of I_{NaL}. Triggered activity in the model can be halted in fibrotic conditions, when myocytes are coupled to fibroblasts. Hence, the mechanism may be more relevant to paroxysmal AF.

1. Introduction

Spontaneous electrical activity of atrial myocytes is linked with the initiation of the most common sustained cardiac arrhythmia, atrial fibrillation (AF). This sustained disease affects 1-2% of the general population, with the prevalence likely to double over the next 50 years (1,2). Although AF is a major cause of morbidity and mortality, clinical treatments for AF are often ineffective, leaving a very costly healthcare problem poorly addressed.

Myocardial sleeves of the pulmonary veins (PVs) near their insertion in the left atrium (LA) are associated with the main source of rapid electrical activity during AF (3,4). The abnormal electrical activity in this region can be maintained by re-entrant circuits of electrical activity, generated due to heterogeneous electrical properties and abrupt changes in myofibre orientation at the PV-LA junctions (5,6). A similar re-entrant substrate exists in the right atrium (RA) (7,8). Re-entry generation requires an initial trigger, which can be provided by ectopic activity in myocytes in the PV sleeves or other atrial cells (4,9). However, mechanisms underlying the emergence of such ectopic triggers are incompletely understood.

The late sodium current, I_{NaL}, can be increased in several cardiac pathologies (10-12). Such increases have recently been proposed to play an important role in arrhythmogenesis. A possible mechanism is through the generation of spontaneous diastolic depolarizations (10), a form of triggered activity where the diastolic membrane potential increases beyond the threshold potential, thus generating one or more spontaneous action potentials (APs). Detailed mechanisms through which the increased I_{NaL} can mediate triggered activity remain unclear.

In this study, we model the increases of I_{NaL} based on experimental data from heart failure (HF) and familiar AF myocytes. Familiar AF is linked with mutations of sodium channels, which result in the increased I_{NaL} (11). HF is one of the major predisposing factors for AF (2): these two conditions often coexist and their intersection creates a vicious circle, with HF promoting the genesis of AF and vice versa. In HF myocytes I_{NaL} is also increased (10, 12). The role of such I_{NaL} increases in triggered activity is explored using electrophysiologically detailed models of atrial cells (13, 14). The contribution of additional factors linked with AF, such as remodeling of outward currents, β-adrenergic stimulation and coupling between myocytes and fibroblasts is also investigated.

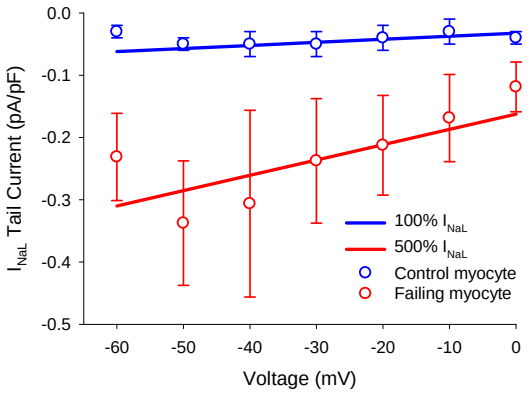

Figure 1. The late Na^+ current, I_{NaL}, is increased 5-fold in HF myocytes (12). Model simulation results (lines) are

plotted against the respective experimental data (dots).

2. Methods

The Ramirez et al. model for the RA cell (13) was used to simulate electrical activity in a canine atrial myocyte. This model includes a passive low-magnitude sodium current ("background Na^+ current"). Conductance of this current was increased 5-fold to model the pathologically enhanced I_{NaL} in HF (Figure 1). Note that such a 5-fold increase in seen in both HF (12) and familial AF (11).

Other pathological conditions associated with AF were considered: (i) 2-fold decreased inward rectifier current, I_{K1}, which is lower in the PV cells compared to atrial myocytes (15); (ii) 1.5-fold increased L-type Ca^{2+} current, I_{CaL}, which is linked with β-adrenergic stimulation (16); (iii) increased electrotonic load on atrial myocytes by fibroblasts, which is linked with fibrosis (17). The latter condition was implemented using the MacCannell et al. model (18) for myocyte-fibroblast electrotonic coupling: in these simulations, each myocyte was coupled with 4 fibroblasts via conductances of 3 nS. The effects of combinations of the above conditions were also explored.

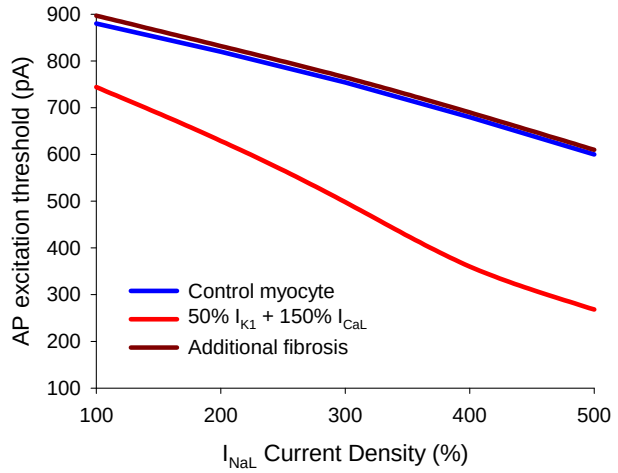

Figure 2. Action potential excitation threshold measured in the canine atrial cell model (13) as a function of I_{NaL}. Three conditions are considered: control cell, pathology associated with triggered activity (50% I_{K1}, 150% I_{CaL}) and the pathology in the presence of additional fibrosis.

In each condition, the AP excitation threshold in the RA cell model was measured as follows. The cell was paced 10 times at a physiological basic cycle length (BCL) of 700 ms by applying pulses (2 ms, −2000 pA) of the stimulating current, I_{stim}. The resultant 10 consecutive APs were then followed after 1000 ms by another I_{stim} pulse (2 ms), the amplitude of which was gradually increased. The minimum I_{stim} amplitude required to initiate an AP was considered the excitation threshold.

Conditions in which triggered activity can be initiated were also investigated using the human atrial cell model by Courtemanche et al. (17). In these simulations, I_{NaL} was increased 5-fold (same as in the canine cell model), and β-adrenergic stimulation was modelled as a collection of multifactorial changes proposed previously (16). Note that the latter also includes a 1.5-fold increase of I_{CaL}.

3. Results

The increase in I_{NaL} leads to a progressive reduction in the AP excitation threshold (Figure 2). In control, a 500% increase of I_{NaL} (seen experimentally in HF, Figure 1), leads to a 30% reduction in the excitation threshold, which is insufficient to generate triggered activity *per se*. Substantial reduction in the excitation threshold can be obtained by incorporating pathological changes: 2-fold decrease of I_{K1} and 1.5-fold increase of I_{CaL} (Figure 2).

Conditions providing the lowest excitation threshold (500% I_{NaL}, 50% I_{K1} and 150% I_{CaL}) were sufficient to initiate triggered activity in form of spontaneous diastolic depolarizations (Figure 3). The latter emerged after the cell was fast-paced at a BCL of 200 ms. The triggered activity lasted 100 s, with a mean period of ~800 ms.

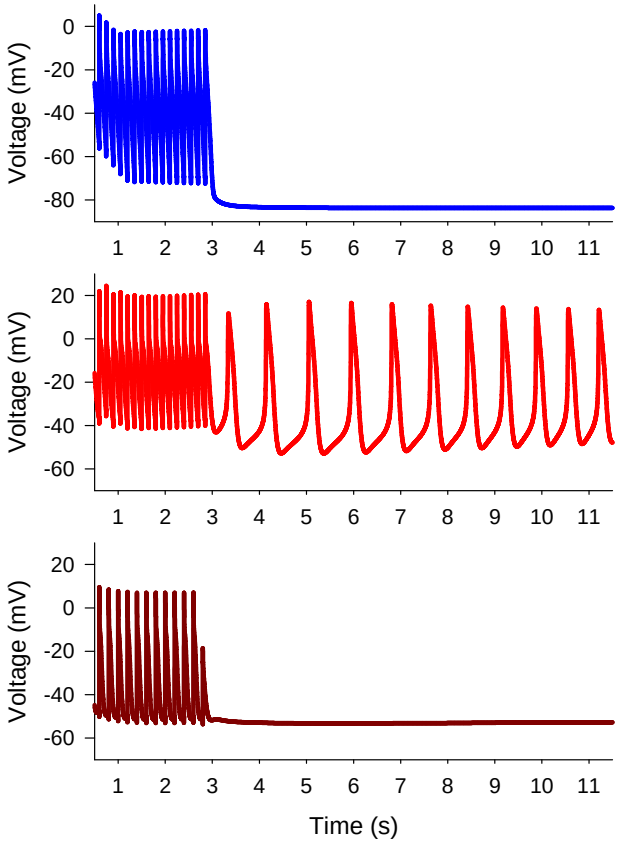

Figure 3. Triggered activity in the canine atrial cell model (13). The cell is initially paced for 3 s at the BCL of 200 ms. Top: Control; Middle: Triggered activity conditions (500% I_{NaL}, 50% I_{K1}, 150% I_{CaL}) result in spontaneous

diastolic depolarizations; Bottom: Additional coupling to fibroblasts halts the diastolic depolarizations.

In conditions when myocytes exhibited triggered activity, additional coupling to fibroblasts resulted in a substantial increase in the excitation threshold (Figure 2) and disappearance of diastolic depolarizations (Figure 3). This may be explained by a reduction in the diastolic potential in a myocyte due to coupling with fibroblasts. In triggered activity conditions, the diastolic potential is increased (Figure 3) − coupling to fibroblasts causes it to decrease, and thus prevents the diastolic depolarizations.

Figure 4 shows that diastolic depolarizations can also be initiated in the human atrial cell model (17) through a combination of the increased I_{NaL} and multifactorial cellular changes due to β-adrenergic stimulation (16).

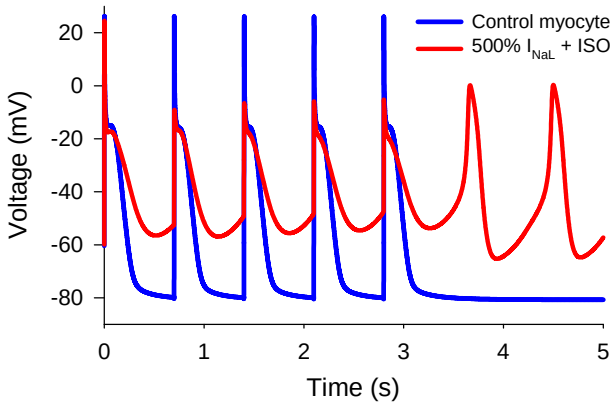

Figure 4. Triggered activity arising in the human atrial cell model (17) due to the increased I_{NaL} and β-adrenergic stimulation (ISO) modelled as described previously (16).

Figure 5 compares the dynamics of AP and underlying ionic currents in control and triggered activity conditions. In conditions that lead to triggered activity, the increased I_{NaL} does not allow the membrane voltage to repolarize fully during diastole, and I_{CaL} is never fully inactivated. These two inward currents lead to a slow increase in the diastolic membrane potential. At approximately -40 mV, the activation gate of I_{CaL} opens, causing a rapid influx of this current that triggers a spontaneous I_{CaL}-driven AP.

More substantial increases of I_{NaL} (over 500%) result in a faster rate of spontaneous diastolic depolarizations. Note that the sodium-calcium exchange current, I_{NaCa}, initially aids the two inward currents (Figure 5). However, it seems to play a secondary role, as triggered activity is still observed (albeit with a slower rate and shorter duration) after I_{NaCa} is set to zero in the model.

The mechanisms of periodic activity in atrial myocytes illustrated in this paper are based on I_{CaL}-driven APs, similar to those observed in the central part of the sino-atrial node (SAN) (18,19). They differ from pacemaking in the SAN in that no specific pacemaking current is required. Instead, the pathologically increased I_{NaL} is responsible for the rise in diastolic potential, activation of I_{CaL} and the generation of spontaneous repetitive APs.

4. Conclusions

We have shown that the increased late sodium current, I_{NaL}, facilitated by the decreased I_{K1} and increased I_{CaL}, can lead to spontaneous triggered activity in atrial cells. All these changes are strongly linked with the genesis of AF (10-12, 15-16). Large pathological increases of I_{NaL}, which is the primarily contributor to triggered activity, can occur in familiar AF (11) and HF (12), a condition frequently associated with AF. The genesis of triggered diastolic depolarizations is facilitated by (i) decreased I_{K1}, which is smaller in the PV compared to RA cells (15,21) and results in a decreased AP excitation threshold, and (ii) β-adrenergic stimulation, which enhances I_{CaL} (16).

The proposed mechanism may be more important in paroxysmal AF. Our simulations show that fibrosis can inhibit triggered activity, which becomes damped by the electrotonic load of fibroblasts coupled to myocytes. Furthermore, ionic remodeling associated with AF leads to a reduction in the density of I_{CaL} and increase in the density of I_{K1} (6,22), which can hinder the proposed mechanism for triggered activity. This is in agreement with the hypothesis that the structural and ionic remodeling of the atria is likely to play a more important role in the maintenance of chronic AF, whereas triggered activity may be more important for AF paroxysms.

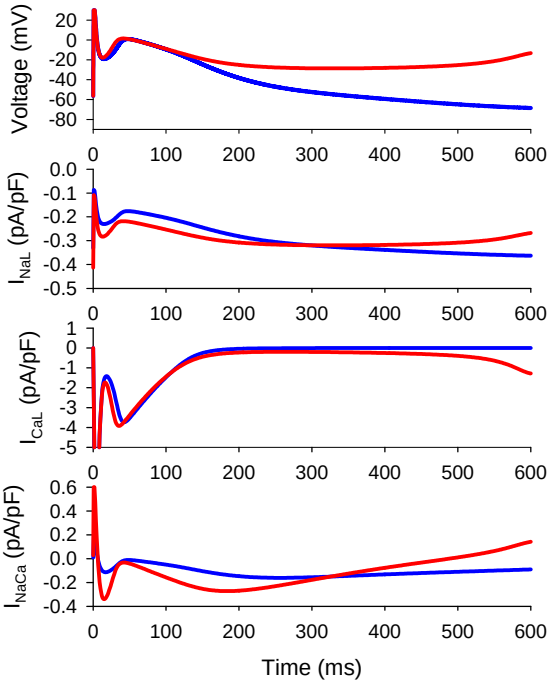

Figure 5. Triggered activity mechanisms. The dynamics of the membrane voltage and several underlying ionic

currents in control (blue lines) and triggered activity (500% I_{NaL}, 50% I_{K1}, 150% I_{CaL}; red lines) are compared.

The conditions of increased I_{NaL} and β-adrenergic stimulation can lead to triggered activity in both canine (13) and human (14) cell models, and hence the proposed mechanism does not depend on a particular model. The simulation results are also in agreement with previous experimental observations that AF in dogs can be (i) initiated by the application isoproterenol (ISO), which is a β-adrenergic agonist and (ii) stopped by the application ranolazine, which is a well-known blocker of I_{NaL} (9). Models with more accurate descriptions of I_{NaL} and I_{NaCa}, and experiments to validate the modelling results are warranted to confirm initial findings of the present study.

Acknowledgements

This research is funded by a grant (PG/10/69/28524) from the British Heart Foundation. We also acknowledge support from the King's College London through the BHF Centre of Research Excellence and the Centre of Excellence in Medical Engineering funded by the Wellcome Trust and EPSRC (WT 088641/Z/09/Z).

References

[1] Stewart S. Cost of an emerging epidemic: an economic analysis of atrial fibrillation in the UK. Heart 2004;90: 286–92.

[2] Anter E, Jessup M, Callans DJ. Atrial fibrillation and heart failure: treatment considerations for a dual epidemic. Circulation 2009; 119: 2516–25.

[3] Haïssaguerre M, Jaïs P, Shah DC, Takahashi A, Hocini M, Quiniou G, et al. Spontaneous initiation of atrial fibrillation by ectopic beats originating in the pulmonary veins. N Engl J Med 1998; 339: 659–66.

[4] Chen S-A, Hsieh M-H, Tai C-T, Tsai C-F, Prakash VS, Yu W-C, et al. Initiation of atrial fibrillation by ectopic beats originating from the pulmonary veins : Electrophysiological characteristics, pharmacological responses, and effects of radiofrequency ablation. Circulation 1999; 100: 1879–86.

[5] Aslanidi OV, Colman MA, Varela M, Zhao J, Smaill BH, Hancox JC, et al. Heterogeneous and anisotropic integrative model of pulmonary veins: computational study of arrhythmogenic substrate for atrial fibrillation. Interface Focus 2013; 3: 20120069.

[6] Colman MA, Varela M, Hancox JC, Zhang H, Aslanidi OV. Evolution and pharmacological modulation of the arrhythmogenic wave dynamics in canine pulmonary vein model. Europace 2014; 16: 416–23.

[7] Aslanidi OV, Colman MA, Stott J, Dobrzynski H, Boyett MR, Holden A V, et al. 3D virtual human atria: A computational platform for studying clinical atrial fibrillation. Prog Biophys Mol Biol 2011; 107: 156–68.

[8] Aslanidi OV, Boyett MR, Dobrzynski H, Li J, Zhang H. Mechanisms of transition from normal to reentrant electrical activity in a model of rabbit atrial tissue: interaction of tissue heterogeneity and anisotropy. Biophys J 2009; 96: 798–817.

[9] Sicouri S, Glass A, Belardinelli L, Antzelevitch C. Antiarrhythmic effects of ranolazine in canine pulmonary vein sleeve preparations. Heart Rhythm 2008;5:1019–26.

[10] Shryock JC, Song Y, Rajamani S, Antzelevitch C, Belardinelli L. The arrhythmogenic consequences of increasing late I_{Na} in the cardiomyocyte. Cardiovasc Res 2013; 99: 600–11.

[11] Savio-Galimberti E, Weeke P, Muhammad R, Blair M, Ansari S, et al. SCN10A/Nav1.8 modulation of peak and late sodium currents in patients with early onset atrial fibrillation. Cardiovasc Res 2014; pii: cvu170.

[12] Valdivia CR, Chu WW, Pu J, Foell JD, Haworth RA, Wolff MR, et al. Increased late sodium current in myocytes from a canine heart failure model and from failing human heart. J Mol Cell Cardiol 2005; 38:475–83.

[13] Ramirez RJ, Nattel S, Courtemanche M. Mathematical analysis of canine atrial action potentials : rate , regional factors , and electrical remodeling. Am J Physiol Hear Circ Physiol 2000; 279: 1522–39.

[14] Courtemanche M, Ramirez RJ, Nattel S. Ionic mechanisms underlying human atrial action potential properties: insights from a mathematical model. Am J Physiol 1998; 275: H301–21.

[15] Ehrlich JR, Cha T-J, Zhang L, Chartier D, Melnyk P, Hohnloser SH, et al. Cellular electrophysiology of canine pulmonary vein cardiomyocytes: action potential and ionic current properties. J Physiol 2003; 551: 801–13.

[16] Grandi E, Pandit S V, Voigt N, Workman AJ, Dobrev D, Jalife J, et al. Human atrial action potential and Ca^{2+} model: sinus rhythm and chronic atrial fibrillation. Circ Res 2011; 109: 1055–66.

[17] Rohr S. Arrhythmogenic implications of fibroblast-myocyte interactions. Circ Arrhythm Electrophysiol 2012; 5: 442–52.

[18] MacCannell KA, Bazzazi H, Chilton L, Shibukawa Y, Clark RB, Giles WR. A mathematical model of electrotonic interactions between ventricular myocytes and fibroblasts. Biophys J 2007; 92: 4121–32.

[19] Butters TD, Aslanidi OV, Inada S, Boyett MR, Hancox JC, Lei M, et al. Mechanistic links between Na+ channel (SCN5A) mutations and impaired cardiac pacemaking in sick sinus syndrome. Circ Res 2010; 107: 126–37.

[20] Chandler N, Aslanidi O, Buckley D, Inada S, Birchall S, Atkinson A, et al. Computer three-dimensional anatomical reconstruction of the human sinus node and a novel paranodal area. Anat Rec 2011; 294: 970–9.

[21] Chen Y-C, Pan N-H, Cheng C-C, Higa S, Chen Y-J, Chen S-A. Heterogeneous expression of potassium currents and pacemaker currents potentially regulates arrhythmogenesis of pulmonary vein cardiomyocytes. J Cardiovasc Electrophysiol 2009; 20: 1039–45.

[22] Cha T-J, Ehrlich JR, Zhang L, Chartier D, Leung TK, Nattel S. Atrial tachycardia remodeling of pulmonary vein cardiomyocytes: comparison with left atrium and potential relation to arrhythmogenesis. Circ 2005; 111: 728–35.

Address for correspondence
Dr Oleg Aslanidi, Division of Imaging Sciences & Biomedical Engineering, King's College London, St Thomas' Hospital London SE1 7EH, UK oleg.aslanidi@kcl.ac.uk